

# All solid-state electric double-layer capacitors based on alkaline polyvinyl alcohol polymer electrolytes

Chun-Chen Yang\*, Sung-Ting Hsu, Wen-Chen Chien

*Department of Chemical Engineering, MingChi University of Technology, Taipei Hsien 243, Taiwan, ROC*

Received 4 January 2005; accepted 4 March 2005

Available online 26 April 2005

## Abstract

Solid-state electrochemical double-layer capacitors (ELDCs) based on alkaline polyvinyl alcohol (PVA) solid polymer electrolytes (SPEs) are prepared. Electrochemical capacitance performance of these capacitors is studied by cyclic voltammetry, galvanostatic charge–discharge testing, and ac impedance spectroscopy. For comparison, two types of EDLC cells are constructed and tested. It is found that an EDLC with a PVA polymer electrolyte exhibits much higher capacitance and longer cycle-life than one with the PP/PE separator. The specific capacitance for the EDLC with the PVA-based SPE is in the range of 100–112 F g<sup>-1</sup>, and depends on the scan rate or the charge–discharge current rates. The results also indicate that the solid-state EDLC shows a relatively stable specific capacitance of 100 F g<sup>-1</sup> after 1000 cycles. The findings suggest that the PVA-based SPE is a promising material for use in EDLCs.

© 2005 Elsevier B.V. All rights reserved.

*Keywords:* Electrochemical double-layer capacitor; Poly vinyl alcohol; Polymer electrolyte; Capacitance

## 1. Introduction

There are two main types of electrochemical capacitor as classified by the charge storage mechanism: (i) electrochemical double-layer capacitor (EDLC), (ii) electrochemical supercapacitor or so-called pseudo-capacitor [1,2]. An EDLC stores energy in the double-layer at the electrode|electrolyte interface, whereas the supercapacitor sustains a Faradaic reaction (or charge-transfer reaction) between the electrode and the electrolyte in a suitable potential window. Activated carbon (AC) materials with high surface area have been used for EDLCs. The high surface area of activated carbon materials is not, however, completely accessible by the electrolyte.

Recently, EDLCs with solid or gel polymer electrolytes have been attracting attention [3–11]. Lewandowski et al. [12] applied an alkaline polyethylene oxide (PEO) solid polymer electrolyte (SPE) to an EDLC and obtained a capacity of

1.7–3.0 F in the potential window of 0–1 V. They also reported a specific capacitance of 93 F g<sup>-1</sup> for a solid-state EDLC based on active carbon. Iwakura et al. [13,14] prepared an alkaline potassium polyacrylate (PAAK) polymer hydrogel electrolyte for an EDLC that delivered a specific capacitance of 142–146 F g<sup>-1</sup> for active carbon material. An alkaline PAA polymer hydrogel electrolyte was also found to give an excellent ionic conductivity of 0.6 S cm<sup>-1</sup> at 25 °C [14].

Alkaline solid polymer electrolytes based on polyethylene oxide (PEO) have been studied for application in nickel–cadmium, nickel–zinc [15,16] and nickel–metal hydride (Ni–MH) battery systems [17,18]. The studies found that an alkaline PEO–KOH polymer electrolyte exhibited an ionic conductivity of around 10<sup>-3</sup> S cm<sup>-1</sup> at room temperature. Yang and Lin prepared an alkaline-blended polymer electrolyte based on PEO–PVA–KOH (PVA = polyvinyl alcohol) for use in Ni–MH [19] and primary Zn–air [20] batteries, and also reported [21,22] a PVA–KOH polymer electrolyte for use application in Ni–MH and Zn–air batteries. Agel et al. [23,24] produced an alkaline anionic exchange

\* Corresponding author.

*E-mail address:* [ccyang@ns1.mit.edu.tw](mailto:ccyang@ns1.mit.edu.tw) (C.-C. Yang).

membrane for fuel cells by grafting quaternary amines on an epichlorohydrin polymer to give ionic conductivities of about  $10^{-2} \text{ S cm}^{-1}$  and with an anionic transport number ( $t^-$ ) greater than 0.9.

Few data have been published on the application of alkaline PVA–KOH polymer electrolytes in EDLCs. This work, therefore, examines the preparation and characteristic capacitance properties of EDLCs using alkaline PVA polymer electrolytes. The capacitance of the solid-state EDLC is evaluated by cyclic voltammetry, galvanostatic charge–discharge cycle test and ac impedance spectroscopy. For comparison, the performance of this EDLC is compared with that of the EDLC with a polypropylene/polyethylene (PP/PE) separator.

## 2. Experimental

### 2.1. Preparation of polymer electrolytes

PVA (molecular weight: 75,000–80,000; Chang-Chung Chemicals) and KOH (Merck) were used as received. The alkaline PVA–KOH polymer electrolytes were prepared by a solution-casting method. Appropriate weight ratios of PVA and KOH were dissolved in water with agitation for about 2–4 h at  $80^\circ\text{C}$ . After complete dissolution of the PVA polymer and KOH powders, the resulting solution was stirred continuously until it took on a homogeneous viscous appearance. The resulting homogeneous solution was poured into a Petri disc and weighed immediately, and then the excess water was evaporated at  $80^\circ\text{C}$  in vacuum oven. After the evaporation, the Petri disc with the PVA–KOH polymer was weighed again. The stable PVA–KOH polymer film was removed and stored in a PE bag until further use.

The conductivities of the alkaline PVA polymer electrolytes were measured by means of the ac impedance method. The electrolytes were sandwiched between SS316 stainless-steel ion-blocking electrodes, each with a surface-area of  $0.785 \text{ cm}^2$ , in a spring-loaded glass holder. A thermocouple was located close to the polymer electrolyte film for temperature measurements. The ac impedance measurements were carried out using an AUTOLAB from Eco Chemi. The frequency range from 1 MHz to 10 Hz at an excitation signal of 10 mV was recorded.

### 2.2. Preparation of porous carbon electrodes

Activated carbon of type BP2000 (Cabot Ltd. Co.) with a specific surface-area of  $1500 \text{ m}^2 \text{ g}^{-1}$  and an average particle size of 15 nm was used as the raw material for the carbon electrodes. The electrode substrate, i.e., the current collector, was prepared from  $1 \times 1$  or  $1 \times 2 \text{ cm}^2$  of Ni-foam. The active carbon (80 wt.%) was mixed with graphite (10 wt.%), and a binder (10 wt.%) of a PTFE aqueous solution or a PVA polymer solution. The resulting mixtures were ground and annealed to obtain a uniform paste by using an ultrasonic bath for at least 2 h. The carbon paste was coated on the nickel foam substrate by a multiple spray and press method to a specified thickness of 0.4–0.5 mm. The resulting porous carbon electrodes were dried under vacuum at  $110^\circ\text{C}$  for 2 h, and then cooled to room temperature for 2 h.

### 2.3. Cell assembly

The configuration of a solid-state EDLC with an alkaline PVA polymer electrolyte (or using a Celgard 5500 PP/PE sep-

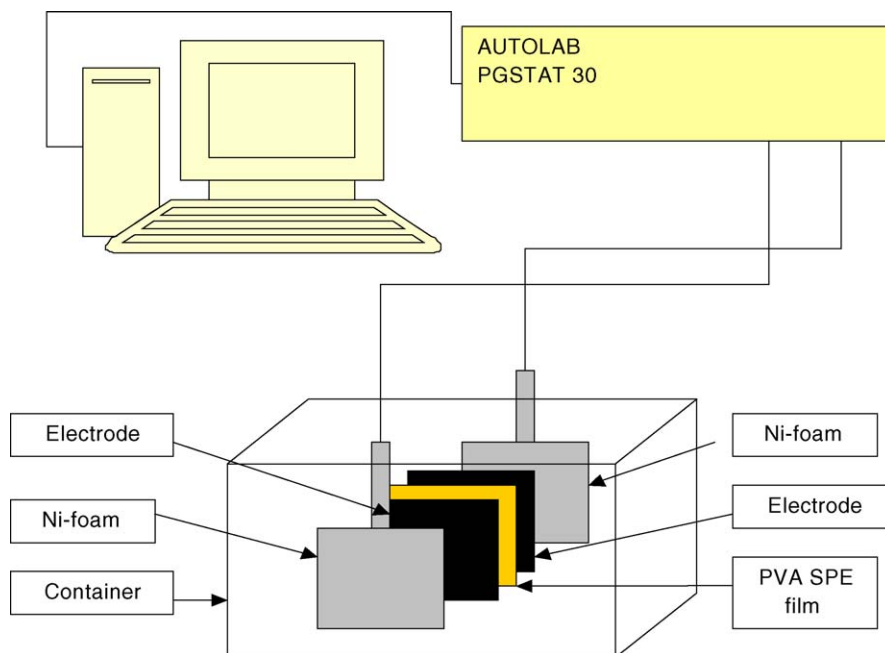


Fig. 1. Configuration of solid-state EDLC capacitor with PVA polymer electrolyte.

arator) is shown schematically in Fig. 1. Two porous carbon electrodes with the same area of  $2\text{ cm}^2$  were cut from a large carbon electrode for assembly of the unit cell. Two porous carbon electrodes and a PVA polymer electrolyte were hot-pressed together for 5 min at  $60\text{ }^\circ\text{C}$ . This lamination process minimizes the ohmic resistance and assures good contact between the carbon electrode and the PVA polymer electrolyte. The PVA polymer electrolyte acts as both a separator and a solid electrolyte.

#### 2.4. Characterization

The surface morphology and microstructure of the porous carbon electrode were examined with a S-2600H scanning electron microscope (Hitachi Co. Ltd.). Cyclic voltammetry, galvanostatic charge–discharge test and the ac impedance spectroscopy were used to examine the electrochemical performance of the solid-state EDLC. The cyclic voltammetry of the porous carbon electrodes was carried out over the po-

tential range of  $-0.8$  to  $0.2\text{ V}$  (versus Hg/HgO) at various scan rates and at  $25\text{ }^\circ\text{C}$ . The galvanostatic charge–discharge test was performed over a cell voltage of  $0$ – $1.1\text{ V}$  at various current densities. The ac impedance analysis was conducted at open-circuit potential over the frequency range of  $1\text{ MHz}$ – $0.01\text{ Hz}$  with an amplitude of  $10\text{ mV}$ .

### 3. Results and discussion

Scanning electron micrographs of the surface morphology of porous carbon electrodes by using the PTFE or PVA polymer solutions as a binder are shown in Fig. 2a and b, respectively. The porous carbon electrode using the PTFE binder shows some cracks and channels on the top surface. In contrast, the porous carbon electrode using the PVA polymer solution binder has considerably fewer cracks and channels on the surface, and therefore, has a much smoother and more uniform morphology.

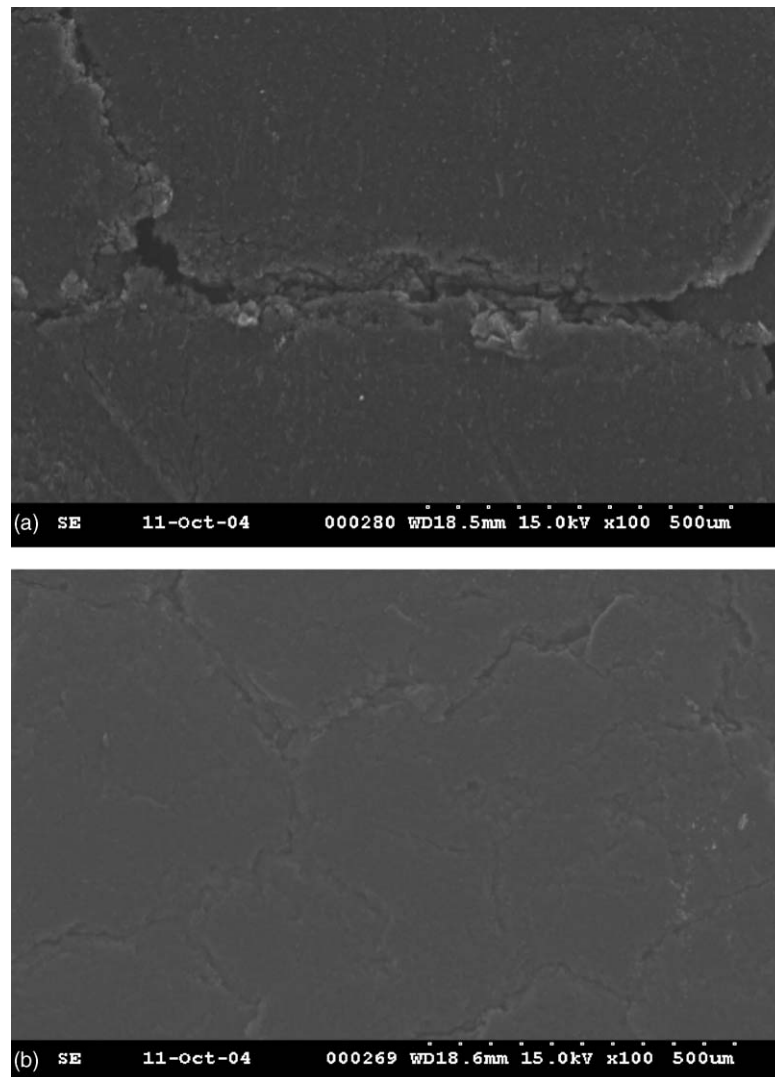


Fig. 2. Scanning electron micrographs of porous carbon electrodes: (a) PTFE binder; (b) PVA binder.

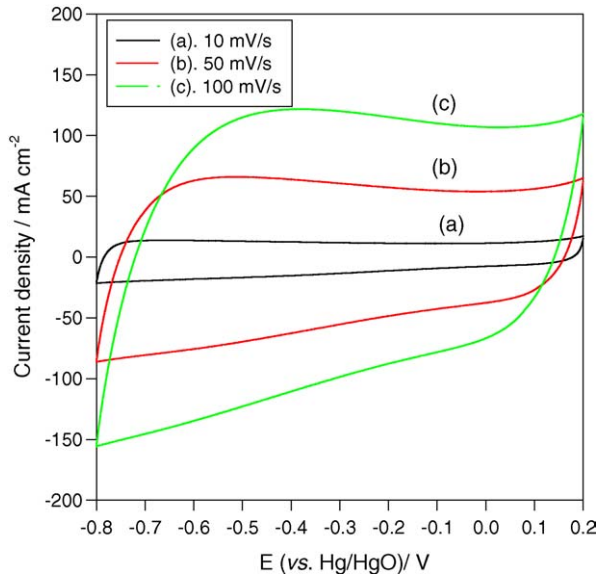


Fig. 3. Cyclic voltammograms for porous carbon electrode in 8M KOH solution at various scan rates at 25 °C.

Cyclic voltammograms for a porous carbon electrode using the PVA polymer solution binder are shown in Fig. 3 and were obtained between potentials of  $-0.8$  and  $0.2$  V at scan rates of  $10$ – $100$   $\text{mV s}^{-1}$  at  $25$  °C. The CV results indicate that the carbon electrode has high capacitance at high scan rates. The carbon electrode shows an ideal rectangular shape, i.e., there is no visible peak from a Faradaic current over the potential region that is scanned. This indicates that charge and discharge occur reversibly at the electrode|electrolyte interface. The charging and discharging capacitance can be estimated using Eqs. (1) and (2). The capacitance calculated from the voltammograms is approximately  $1.245$  F, which corresponds to  $115$   $\text{F g}^{-1}$  of BP200 activated carbon material. (Note: the specific capacitance was calculated with respect to the mass of the activated carbon material only).

$$C_{\text{cell}}(F) = \frac{dQ}{dE} = I \frac{dt}{dE} = \frac{I}{dE/dt} = \frac{I}{\nu} \quad (1)$$

$$C_{\text{spec}} \left( \frac{F}{g} \right) = \frac{2C_{\text{cell}}}{m} \quad (2)$$

where  $C_{\text{cell}}$ ,  $Q$ ,  $I$ ,  $\nu$  and  $E$  are the capacitance (F), the total charge (C), the charging/discharging current (A), the scan rate ( $\text{V s}^{-1}$ ) and the cell potential difference (V), respectively.  $C_{\text{spec}}$  and  $m$  are the specific capacitance of the EDLC ( $\text{F g}^{-1}$ )

Table 1

Capacitance of porous carbon electrodes at 25 °C

Rate ( $\text{mV s}^{-1}$ )	Total capacitance by CV method (F)		Specific capacitance ( $C_{\text{spec}}$ ) ( $\text{F g}^{-1}$ )	
	Charge	Discharge	Charge	Discharge
10	1.334	1.245	123.1	115.3
50	1.113	1.101	103.2	102.7
100	1.001	0.994	92.93	92.27

Note:  $m = 0.01$  g in electrode with surface area of  $1$   $\text{cm}^2$ .

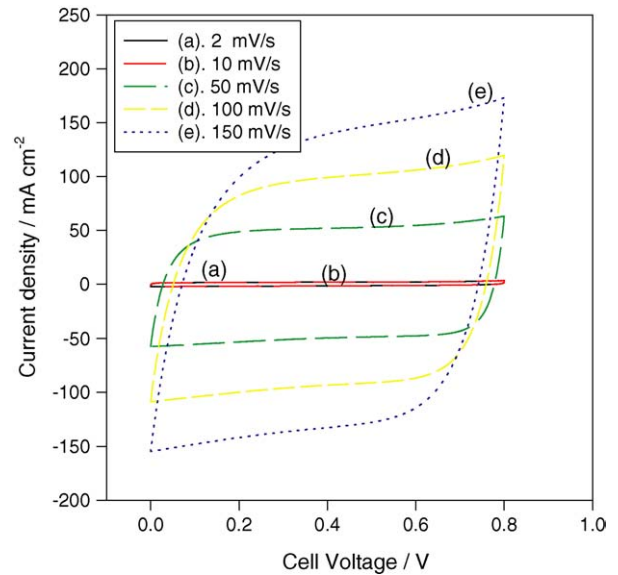


Fig. 4. CV curves for EDLC with PVA polymer electrolyte at different scan rates at 25 °C.

and the mass of activated carbon in the electrode. Electrochemical capacitance values are listed in Table 1 for porous carbon electrodes using a PVA polymer solution binder at different scan rates at 25 °C.

Cyclic voltammograms are shown in Fig. 4 for a unit EDLC with the PVA polymer electrolyte over a potential of  $0$ – $0.8$  V at scan rates of  $2$ – $150$   $\text{mV s}^{-1}$  at  $25$  °C. The data clearly indicate that the solid-state EDLC exhibits a high capacitance at high scan rates. The shape of the voltammograms is close to an ideal rectangular one; there are no visible peaks in the  $0$ – $0.8$  V potential range. This also indicates that charge/discharge of the EDLC occurs almost reversibly at the electrode|polymer electrolyte interface. Some characteristic properties of the EDLC with PVA polymer electrolyte at different scan rates at 25 °C are given in Table 2.

Cyclic voltammograms for the EDLC at different terminal potentials from  $0.8$  to  $1.1$  V at a scan rate of  $10$   $\text{mV s}^{-1}$  at  $25$  °C are given in Fig. 5. There, at a terminal potential of  $1.1$  V, the CV is rather stable for charge and discharge. It can be concluded that the useful potential window for the EDLC can be extended to  $1.1$  V without any significant distortion to the CV curve. The capacitance calculated from the voltammograms is about  $1.06$  F, which corresponds to  $100$   $\text{F g}^{-1}$  of BP200 activated carbon material.

Table 2  
Capacitance values for EDLCs with PVA SPE at 25 °C

Rate (mV s <sup>-1</sup> )	Total capacitance by CV method (F)		Specific capacitance ( $C_{\text{spec}}$ ) (F g <sup>-1</sup> )	
	Charge	Discharge	Charge	Discharge
10	1.1394	1.0663	105.78	98.99
50	1.0748	1.0545	99.78	97.90
100	0.9926	0.9784	92.16	90.83

Note:  $m = 0.02$  g in electrode with surface area of 2 cm<sup>2</sup>.

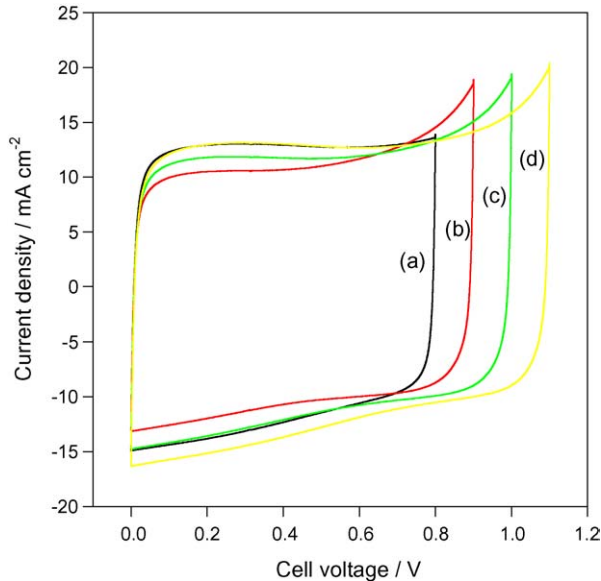


Fig. 5. CV curves for EDLC with PVA polymer electrolyte at different terminal potentials at a scan rate of 10 mV s<sup>-1</sup>: (a) 0–0.8 V; (b) 0–0.9 V; (c) 0–1.0 V; (d) 0–1.1 V.

Cyclic voltammograms are presented in Fig. 6 for a unit EDLC with a Celgard PP/PE separator over the potential range of 0–0.8 V at scan rates of 2–100 mV s<sup>-1</sup> at 25 °C. The EDLC exhibits a higher capacitance when the scan rate is increased. The voltammograms are severely distorted (not rectangular) and there are also no visible peaks in the 0–0.8 V potential window. Thus, the charge/discharge of the EDLC is not perfectly reversibly at the electrode–separator interface. Some characteristic properties of the EDLC with the PP/PE separator at different scan rates at 25 °C are summarized in Table 3.

The galvanostatic charging and discharging curves of the EDLC with a PVA polymer electrolyte at different charge currents from 10 to 100 mA are shown in Fig. 7. The EDLC

Table 3  
Capacitance values for EDLCs with PP/PE separators at 25 °C

Rate (mV s <sup>-1</sup> )	Total capacitance by CV method (F)		Specific capacitance ( $C_{\text{spec}}$ ) (F g <sup>-1</sup> )	
	Charge	Discharge	Charge	Discharge
10	0.6631	0.5740	61.57	53.29
50	0.3286	0.3095	30.51	28.73
100	0.2489	0.2371	23.11	22.02

Note:  $m = 0.02$  g in electrode with surface area of 2 cm<sup>2</sup>.

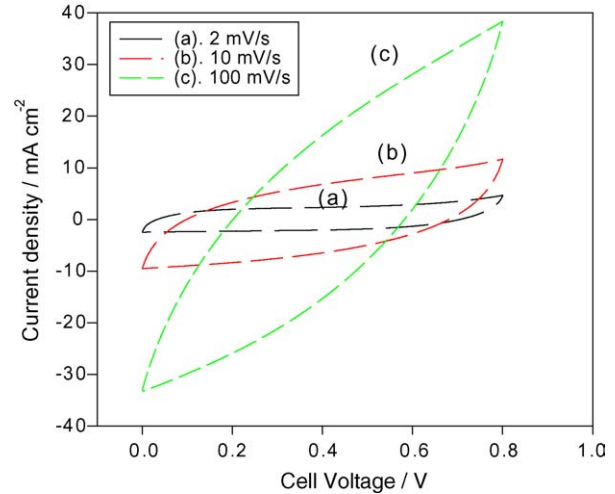


Fig. 6. CV curves for EDLC with PP/PE separator at different scan rates and 25 °C.

displays typical charge–discharge performance with a very low ohmic resistance at the potential switching point. The charging and discharging capacitance can be estimated from:

$$C_{\text{cell}}(F) = \frac{Q}{\Delta E} = \frac{(I \times t)}{\Delta E} \quad (3)$$

where  $C_{\text{cell}}$ ,  $I$ ,  $t$  and  $E$  are the capacitance (F), the charge–discharge current (A), the charge–discharge time (s) and the cell potential difference (V), respectively. The capacitance from the charge–discharge curve (112.5 F g<sup>-1</sup>) is much greater than that determined from cyclic voltammetry (99 F g<sup>-1</sup>).

For comparison, the galvanostatic charge–discharge curves for EDLCs with a PVA polymer electrolyte and the PP/PE separator are compared in Fig. 8. Obviously, the performance for the EDLC with the PVA SPE is much better than that of the EDLC with the PP/PE separator. The latter exhibits a large ohmic drop at the potential switching

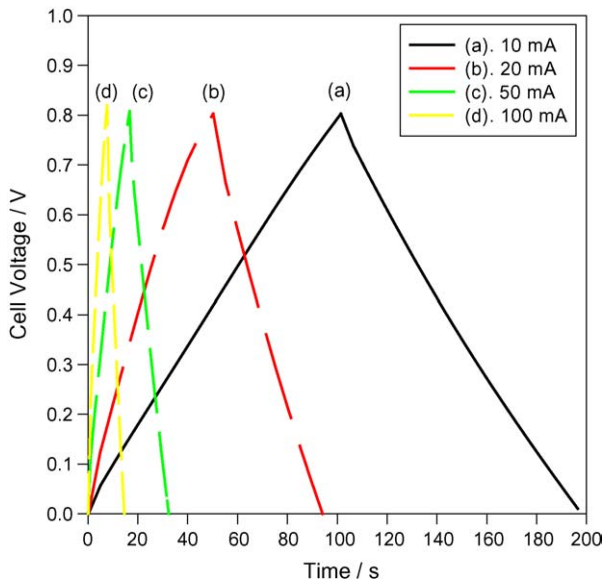


Fig. 7. Charge–discharge curves for EDLC with PVA polymer electrolyte at different charge–discharge rates and at 25 °C.

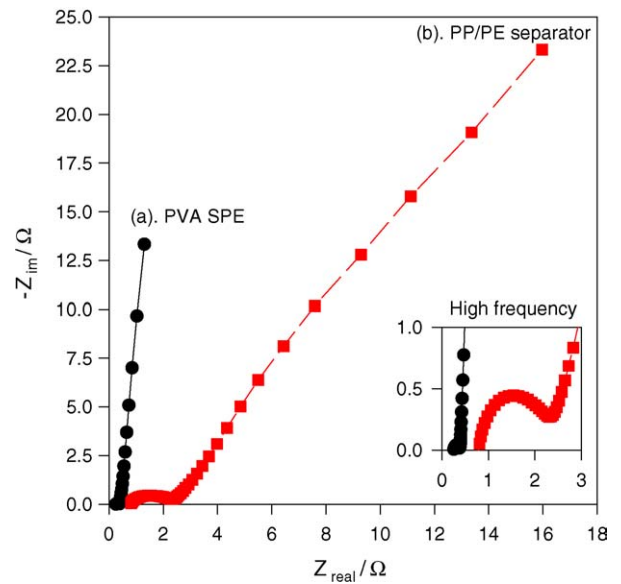


Fig. 9. ac impedance spectra for EDLCs with PVA SPE and with PP/PE separator.

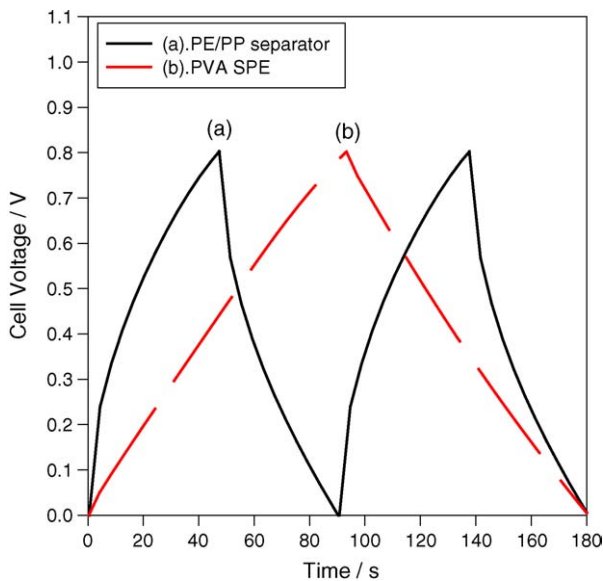


Fig. 8. Charge–discharge curves for EDLCs with: (a) PVA polymer electrolyte; (b) PP/PE separator at 25 °C. Charge–discharge current at 10 mA; area = 2 cm<sup>2</sup>.

point, but the former does not show any ohmic drop during the charge–discharge cycle. The specific capacitance for the EDLC with the PP/PE separator is only about 53 F g<sup>-1</sup> from the CV method, but is 62.8 F g<sup>-1</sup> from the galvanostatic charge–discharge method. Using a PVA polymer electrolyte a PVA polymer binder, the capacitance of the EDLC is greatly enhanced due to the excellent hydrophilic property of the PVA polymer.

The ac impedance method was also used to calculate the specific capacitance and the bulk resistance ( $R_b$ ), of the EDLCs. The spectra (i.e., Nyquist plot) for an EDLC with a PVA polymer electrolyte and one with a P/PE separator are presented in Fig. 9. The spectra display a small semicircle at high frequency (inset) followed by a transition to linearity at low frequency. At high frequency, the spectral feature represents a limiting diffusion process and at low frequency it represents purely capacitive characteristic. The ac spectrum for the EDLC with the PVA SPE displays a vertical line close to 90° at low frequency, which indicates purely capacitive behavior. On the other hand, the ac spectrum for the EDLC with the PP/PE separator has a line close to 45° in the low-frequency range. It is typical of Warburg impedance (a limiting diffusion process), and is not useful for a capacitor to

Table 4  
Characteristic parameters for EDLCs at 25 °C

Types	ac parameters		Specific capacitance by CV method (F g <sup>-1</sup> )		Specific capacitance by charge–discharge method (F g <sup>-1</sup> )		Time constant ( $\tau = R_s C$ ) (s)	SE (Wh kg <sup>-1</sup> )	SP (kW kg <sup>-1</sup> )
	$R_s$ (ohm)	$R_p$ (ohm)	Charge	Discharge	Charge	Discharge			
EDLC cell with PVA SPE	0.251	0.138	105.78	98.99	117.75	112.48	0.3	10.0	29.61
EDLC cell with PP/PE separator	0.945	3.772	61.57	53.29	69.81	62.86	0.6	5.6	7.86

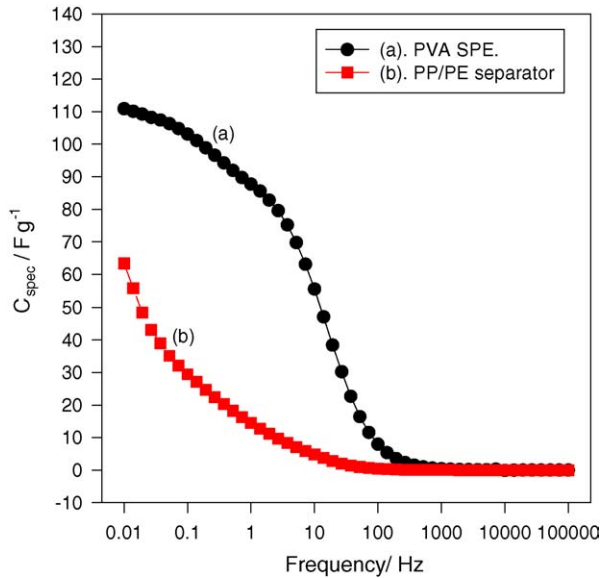


Fig. 10. Capacitance vs. frequency by ac impedance method for EDLC with PVA SPE at 25 °C.

store charge. The internal resistances ( $R_b$ ) of EDLCs with the PVA SPE and the PP/PE separator are estimated to be 0.138 and 3.77 ohm, respectively. The time constant ( $\tau = C_{\text{cell}}R_b$ ) is about 0.3 and 0.6 s for the EDLC with the PVA SPE and with the PP/PE separator, respectively. The low values of time constant illustrate the good power capability of the EDLCs. From the ac data, the EDLC assembled with the PVA polymer electrolyte does indeed exhibit a much higher characteristic capacitance.

Some characteristic parameters for EDLCs with the PVA SPE and with the Celgard 5500 PP/PE separator are listed in Table 4. The specific energy (SE) and specific power (SP) are calculated from:  $SE = 1/2(CV^2)$  and  $SP = 1/4(V^2R^{-1})$ , respectively. The SE and SP for the EDLC with the PVA SPE are both higher than those for the EDLC with the Celgard 5500 PP/PE separator, i.e.,  $10 \text{ W kg}^{-1}$  versus  $5.6 \text{ W kg}^{-1}$  and  $29.6 \text{ kW kg}^{-1}$  versus  $7.8 \text{ kW kg}^{-1}$ , respectively.

The capacitance–frequency dependence of EDLCs with the PVA SPE or the PP/PE separator, as from ac impedance measurements, is demonstrated in Fig. 10. The specific capacitance for EDLCs from ac spectra can be calculated by using the following relationship:

$$C_{\text{cell}} = \frac{1}{-2\pi f Z''} = -(2\pi f Z'')^{-1} \quad (4)$$

where  $Z''$  is the imaginary impedance (ohm) and  $f$  the frequency (Hz). The specific capacitance for the EDLC with the PVA SPE is about  $110 \text{ F g}^{-1}$ , but is only about  $65 \text{ F g}^{-1}$  for the EDLC with the PP/PE separator. The capacitance results from the ac impedance method are consistent with those obtained from the galvanostatic charge–discharge method.

The variation of the specific capacitance with cycle number is given in Fig. 11. The cycle-life stability test is conducted by galvanostatic charge–discharge cycling at a constant cur-

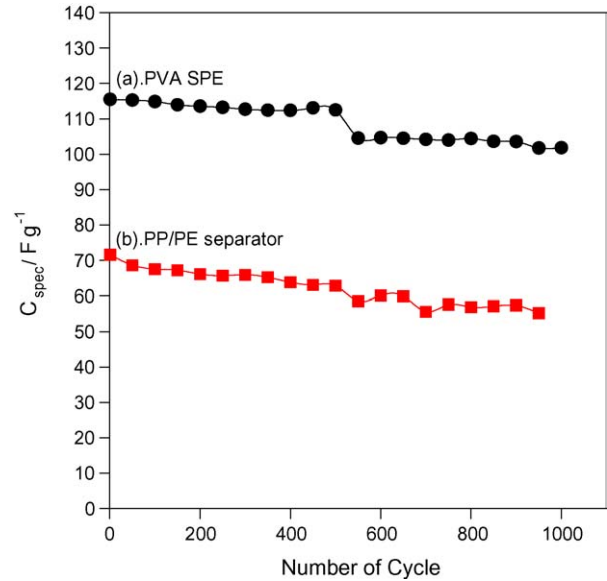


Fig. 11. Cycle-life results for EDLCs with PVA SPE and with PP/PE separator.

rent of 10 mA (i.e.,  $i = 5 \text{ mA cm}^{-2}$ ). The specific capacitance of the EDLC with the PVA SPE after 1000 cycles is still about  $100 \text{ F g}^{-1}$ , but is only about  $60 \text{ F g}^{-1}$  for the EDLC with the PP/PE separator.

The relationships between the mass and the area-specific capacitances and the current density are shown in Fig. 12. The ability of the EDLC to discharge at a high rate is of great importance for practical use. Clearly, the results indicate that the EDLC has a high rate capacitance at a low discharge current density; conversely, it has a low capacitance at a high discharge current density. These features may be due to the diffusion-limiting process of the highly porous nano-structure of the BP2000 carbon material used in the

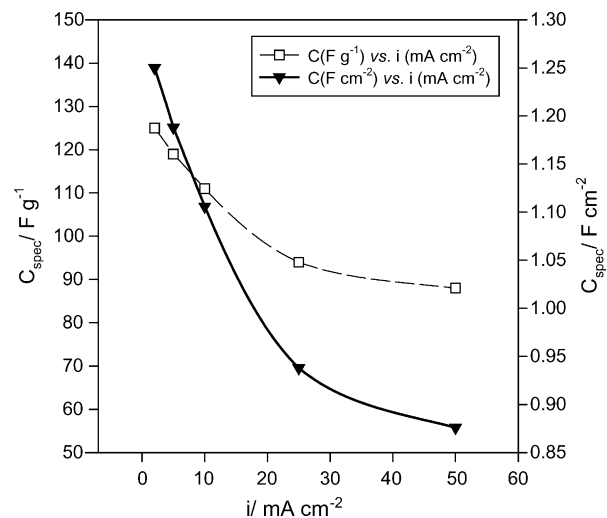


Fig. 12. Specific capacitance of EDLC with PVA SPE as function of discharge current density at 25 °C.

electrode. The performance of the EDLC reaches a limiting value of  $90 \text{ F g}^{-1}$  when the discharge rate is greater than  $50 \text{ mA cm}^{-2}$ . This demonstrates that the EDLC with the PVA SPE has an excellent high power capability.

#### 4. Conclusions

An alkaline PVA polymer electrolyte with a high ionic conductivity of the order of  $10^{-2} \text{ S cm}^{-1}$  has been used in a solid-state capacitor (ELDC). The electrochemical capacitances of EDLCs with PVA polymer electrolytes and the PP/PE separators have been evaluated by means of cyclic voltammetry galvanostatic charge–discharge test, and ac impedance spectroscopy. The EDLC with the PVA SPE has higher capacitance than that with the PP/PE separator. This may be due to the hydrophilic property of the PVA polymer used as a binder and a solid electrolyte in the EDLC. The experimental data also indicate that the EDLC with the PVA SPE has rather stable and good cycle-life characteristics. Accordingly, the alkaline PVA polymer electrolyte is a promising material for solid-state capacitors.

#### Acknowledgement

Financial support for the research project from the National Science Council, Taiwan, ROC (Contract No: NSC-92-2214-E-131-001) is gratefully acknowledged.

#### References

- [1] A. Burke, *J. Power Sources* 91 (2000) 37.
- [2] R. Kotz, M. Carlen, *Electrochim. Acta* 45 (2000) 2483.
- [3] A. Rudge, I. Raistrick, S. Gottesfeld, J.P. Ferraris, *Electrochim. Acta* 39 (1994) 273.
- [4] X. Liu, T. Osaka, *J. Electrochem. Soc.* 143 (1996) 3982.
- [5] T. Osaka, X. Liu, M. Nojima, T. Momma, *J. Electrochem. Soc.* 146 (1999) 1724.
- [6] Y.G. Wang, X.G. Zhang, *Electrochim. Acta* 49 (2004) 1957.
- [7] K.W. Park, H.J. Ahn, Y.E. Sung, *J. Power Sources* 109 (2002) 500.
- [8] P. Sivaraman, V.R. Hande, V.S. Mishra, S. Rao Ch, A.B. Samui, *J. Power Sources* 124 (2003) 351.
- [9] C. Kim, K.S. Yang, W.J. Lee, *Electrochem. Solid-State Lett.* 7 (8) (2004) A247.
- [10] N. Miura, S. Oonishi, K.R. Prasad, *Electrochem. Solid-State Lett.* 7 (11) (2004) A397.
- [11] K. Kierzek, E. Frackowiak, G. Lota, G. Gryglewicz, J. Machnikowski, *Electrochim. Acta* 49 (2004) 515.
- [12] A. Lewandowski, M. Zajder, E. Frackowiak, F. Beguin, *Electrochim. Acta* 46 (2001) 2777.
- [13] C. Iwakura, H. Wada, S. Nohara, N. Furukawa, H. Inoue, M. Morita, *Electrochem. Solid-State Lett.* 6 (2) (2003) A37.
- [14] H. Wada, S. Nohara, N. Furukawa, H. Inoue, N. Sugoh, H. Hideharu, M. Morita, C. Iwakura, *Electrochim. Acta* 49 (2004) 4871.
- [15] J.F. Fauvarque, S. Gunot, N. Bouzir, E. Salmon, J.F. Penneau, *Electrochim. Acta* 40 (1995) 2449.
- [16] S. Gunot, E. Salmon, J.F. Penneau, F. Fauvarque, *Electrochim. Acta* 43 (1998) 1163.
- [17] N. Vassal, E. Salmon, F. Fauvarque, *Electrochim. Acta* 45 (2000) 1527.
- [18] N. Vassal, E. Salmon, J.F. Fauvarque, *J. Electrochem. Soc.* 146 (1999) 20.
- [19] C.C. Yang, *J. Power Sources* 109 (2002) 22.
- [20] C.C. Yang, S.J. Lin, *J. Power Sources* 112 (2002) 497.
- [21] C.C. Yang, S.J. Lin, *Mater. Lett.* 57 (2002) 873.
- [22] C.C. Yang, S.J. Lin, *J. Appl. Electrochem.* 33 (2003) 777.
- [23] E. Agel, J. Bouet, J.F. Fauvarque, H. Yassir, *Ann. Chim. -Sci. Mat.* 26 (2001) 59.
- [24] E. Agel, J. Bouet, J.F. Fauvarque, *J. Power Sources* 101 (2001) 267.